

Electronic Supplementary Information

Photocatalytic oxygen evolution triggered by photon upconverted emission based on triplet-triplet annihilation

Yosuke Kageshima,^{*ab} Shutaro Tateyama,^a Fuminao Kishimoto,^c Katsuya Teshima,^{ab}
Kazunari Domen^{bd} and Hiromasa Nishikiori^{*ab}

^a Department of Materials Chemistry, Faculty of Engineering, Shinshu University, 4-17-1 Wakasato, Nagano 380-8553, Japan.

^b Research Initiative for Supra-Materials (RISM), Shinshu University, 4-17-1 Wakasato, Nagano 380-8553, Japan.

^c Department of Chemical System Engineering, School of Engineering, The University of Tokyo, 7-3-1 Hongo, Bunkyo-ku, Tokyo 113-8656, Japan.

^d Office of University Professors, The University of Tokyo, 7-3-1 Hongo, Bunkyo-ku, Tokyo 113-8656, Japan.

Table S1. The mass-based percentages of C, H and N in the dye-clay composites as determined by the CHN analyses, and the associated C/N molar ratios.

	C / wt%	H / wt%	N / wt%	C/N molar ratio
CTAB-Kunipia	26.96	5.47	1.75	18.0
CTAB-Sumecton	31.68	6.43	2.05	18.0
DPA-PtOEP-Kunipia	27.85	5.43	1.73	18.8
DPA-PtOEP-Sumecton	31.86	6.49	2.07	17.9

Table S2. The calculated amounts of DPA and PtOEP intercalated into the host clay materials and molar ratio of PtOEP to DPA.

	DPA ^[a] / $\mu\text{mol g}^{-1}$	PtOEP ^[b] / nmol g^{-1}	PtOEP/DPA ratio
DPA-PtOEP-Kunipia	78.3	0.71	9.1×10^{-6}
DPA-PtOEP-Sumecton	10.7	0.42	3.9×10^{-5}

[a] Amounts of DPA per weight of the host clay material determined from the light absorption of the DPA remaining in the TL after solvothermal treatment. [b] Amounts of PtOEP per weight of the host clay material determined from the light absorption of the PtOEP remaining in the TL after solvothermal treatment. Amounts of the dyes are quite small compared with CTAB.

Electronic Supplementary Information

The XRD patterns for bare Kunipia and CTAB-Kunipia specimens prepared using a conventional cation exchange method are presented in Fig. S1. The bare Kunipia generated a diffraction peak at $2\theta = 7.10^\circ$, corresponding to 1.25 nm spacing between neighboring aluminosilicate layers.¹ In contrast, the CTAB-Kunipia prepared by the conventional method produced peaks at $2\theta = 2.22^\circ$, 4.48° , 6.79° and 9.02° , corresponding to the second, third and fourth-order diffractions, respectively, associated with a spacing of 3.98 nm.

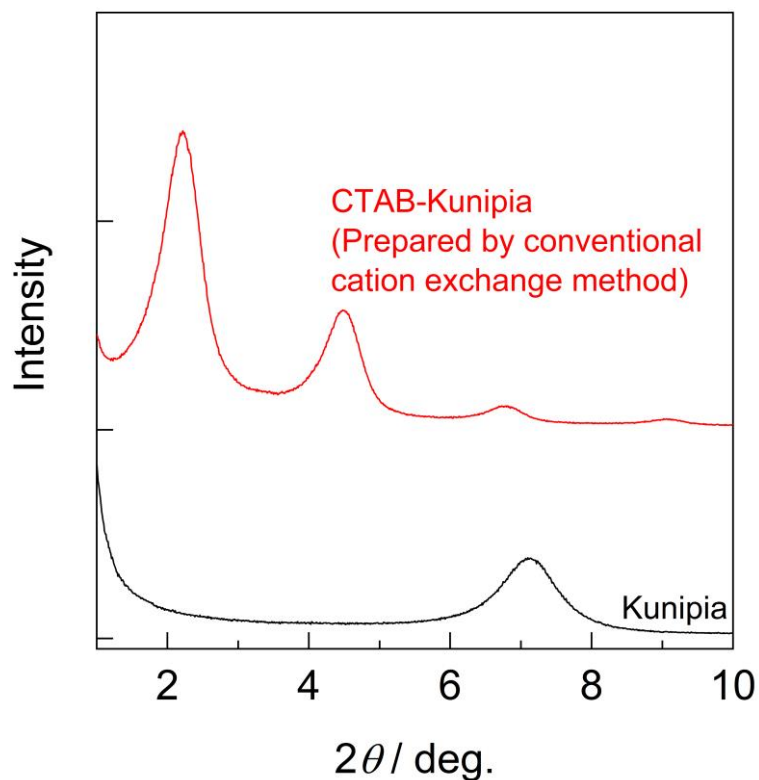


Fig. S1. The XRD patterns obtained from Kunipia and CTAB-Kunipia samples prepared by a conventional cation exchange method.

Electronic Supplementary Information

The TG-DTA data for the bare Kunipia and CTAB-Kunipia specimens prepared using a conventional cation exchange method as well as the solvothermal method are presented in Fig. S2. The mass loss evident below 100 °C is attributed to the evaporation of adsorbed water. The CTAB-Kunipia also exhibited additional mass loss above 200 °C that is assigned to the decomposition of the CTAB. Because the mass loss due to the decomposition of CTAB was equivalent to 41.9%, the CTAB loading was calculated to be 2.54 mmol CTAB per gram of clay, considering that the molecular weight of CTA⁺ is 284.5 g mol⁻¹. The amount of CTAB was thus far in excess of the CEC of montmorillonite (119 meq/100 g of Kunipia¹), possibly because the surfactant formed a multilayer structure, similar to a previously reported phenomenon.² Therefore, it appears that the CTAB intercalated using the conventional cation exchange technique was equivalent to almost the full CEC of the Kunipia. Meanwhile, approximately 31.9% of weight loss was confirmed for the case of CTAB-Kunipia prepared through the solvothermal technique.

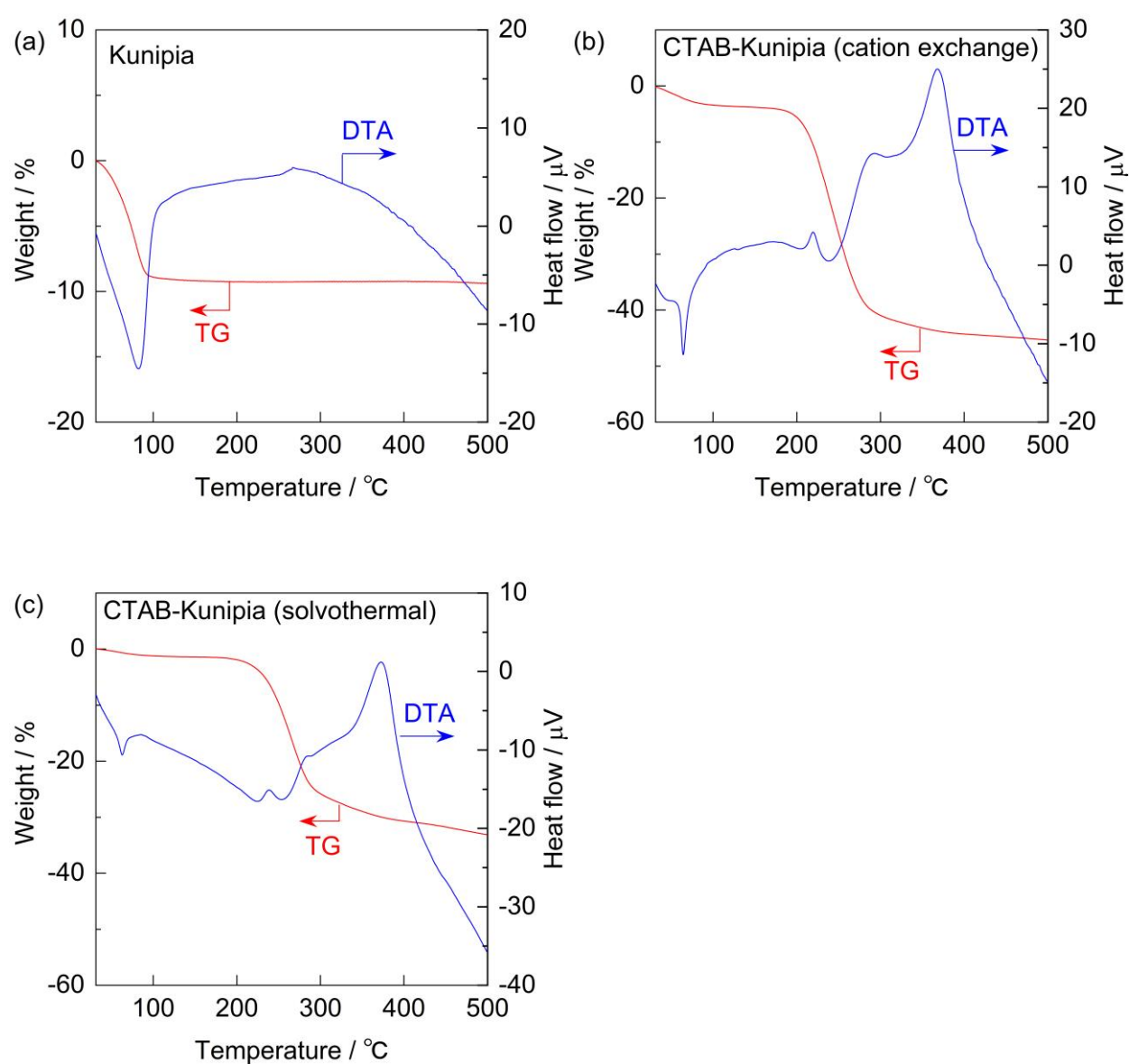


Fig. S2. TG-DTA curves for (a) bare Kunipia, (b) CTAB-Kunipia prepared by a conventional cation exchange method, and (c) CTAB-Kunipia prepared by the solvothermal method.

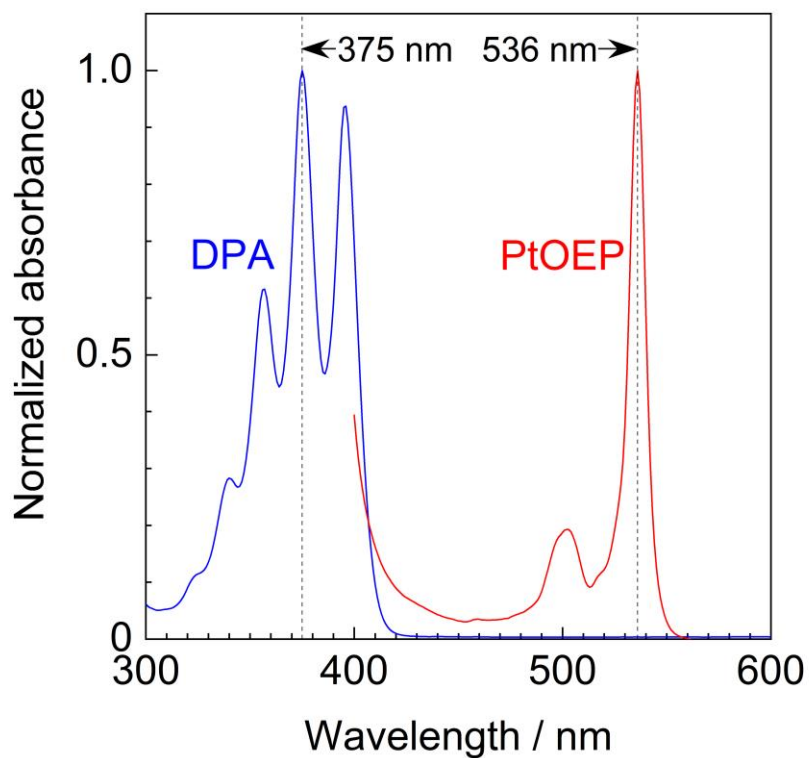


Fig. S3. Normalized absorption spectra for DPA (0.1 mM) and PtOEP (5 μ M) in TL solutions.

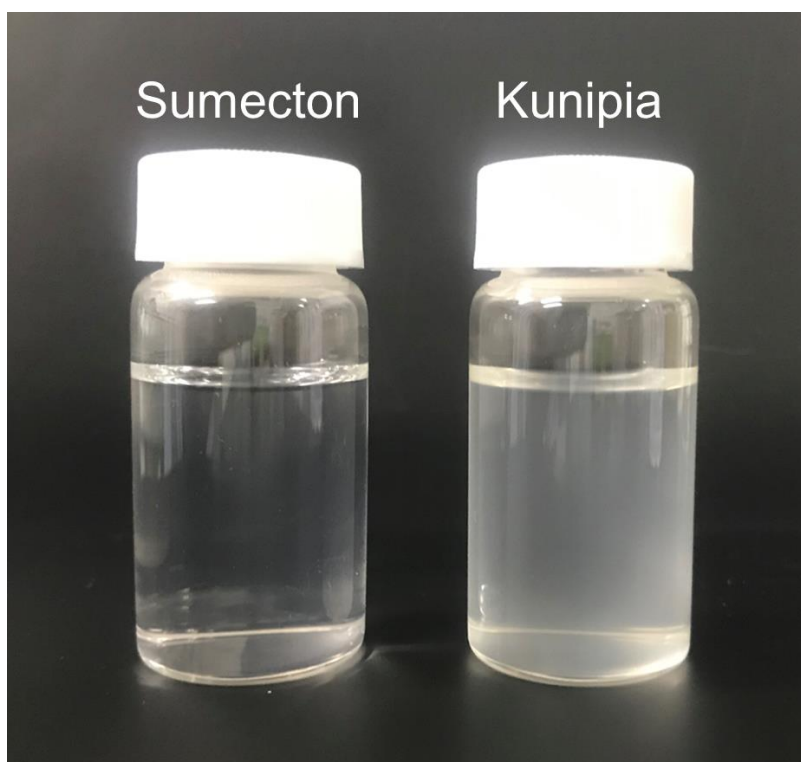


Fig. S4. Photographic image of Sumecton or Kunipia dispersed in water with concentration of 1 g of clay per 1 L of water.

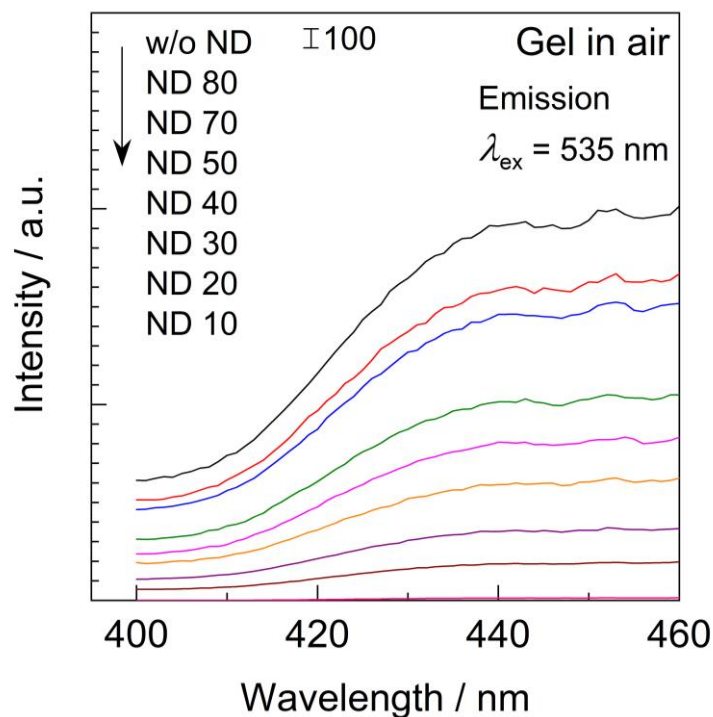


Fig. S5. Emission spectra of DPA-PtOEP-Sumecton in the form of a wet gel in air at various excitation intensities.

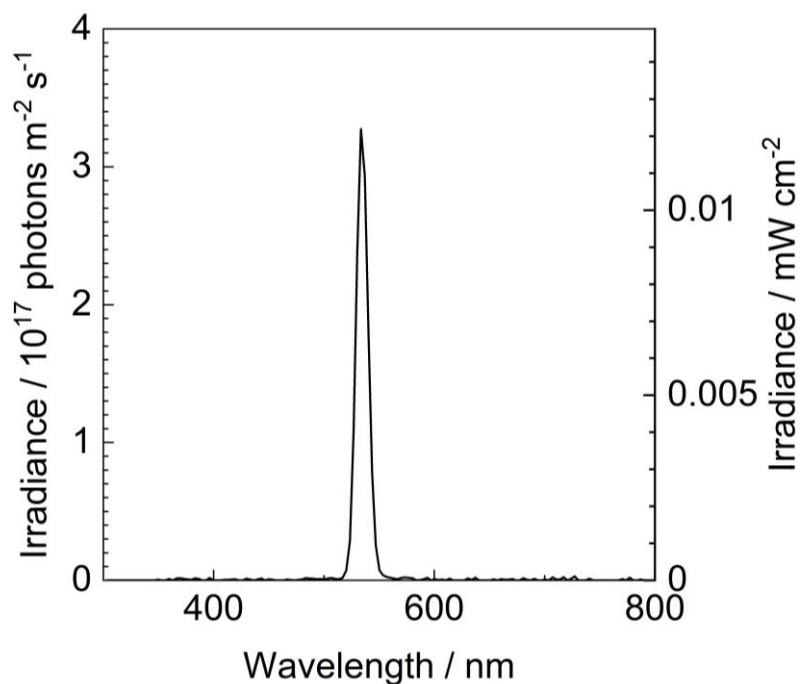


Fig. S6. The output of the light source (150 W Xe lamp equipped with a monochromator in the fluorescence spectrophotometer) utilized to determine the photon flux dependence of the emission intensity. Since the present light source was sharp monochromatic light, the spectra in the unit of “photons $\text{m}^{-2} \text{ s}^{-1}$ (left axis)” and “ mW cm^{-2} (right axis)” showed the almost same shape.

Electronic Supplementary Information

We estimated the apparent quantum yield (AQY) for converting green light ($\lambda_{\text{ex}} = 535 \text{ nm}$) to a blue emission ($\lambda_{\text{em}} = 430 \text{ nm}$), since it should be difficult to accurately estimate the “adsorbed photon number” in the present particulate system. The light intensity at 430 and 535 nm monitored using the present fluorescence spectrophotometer were first calibrated with using a spectroradiometer to convert the “intensity” to “photon flux” at the wavelength as summarized in Fig. S7a and S7b. The upconverting emission intensity of the DPA-PtOEP-Sumecton was then calculated into the unit of “photon $\text{cm}^{-2} \text{s}^{-1} \text{nm}^{-1}$ ” as shown in Fig. S7c. The AQY with emitting 430 nm of light was unfortunately quite low equivalent to less than 0.01%. This quite low AQY also hampered to measure the fluorescence lifetime.

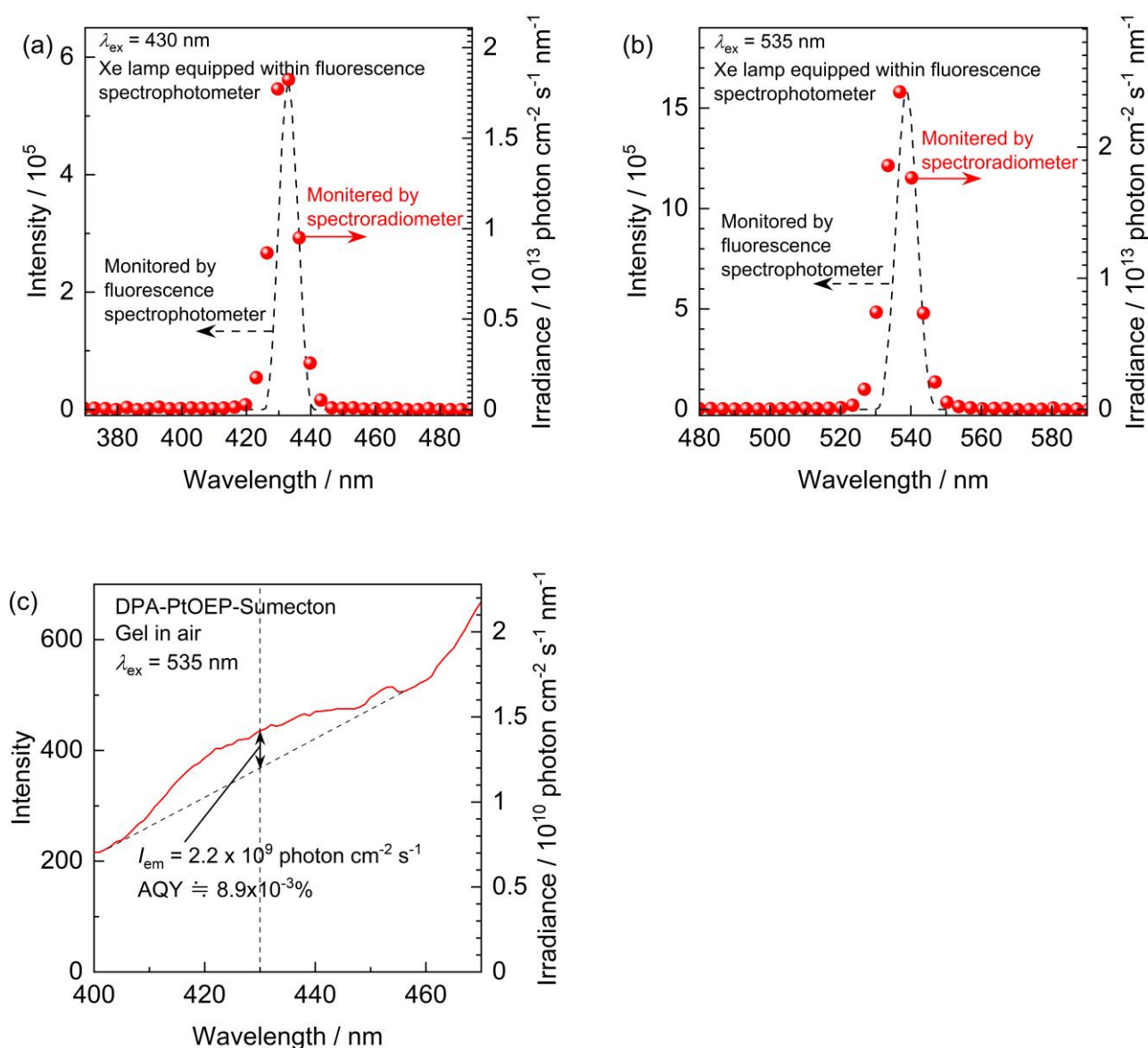


Fig. S7. The spectra of the monochromatic light at (a) 430 and (b) 535 nm of wavelength generated by the Xe lamp equipped in the fluorescence spectrophotometer detected by the same spectrophotometer or the spectroradiometer. (c) Emission spectrum of DPA-PtOEP-Sumecton in the unit of “intensity” and “photon flux”.

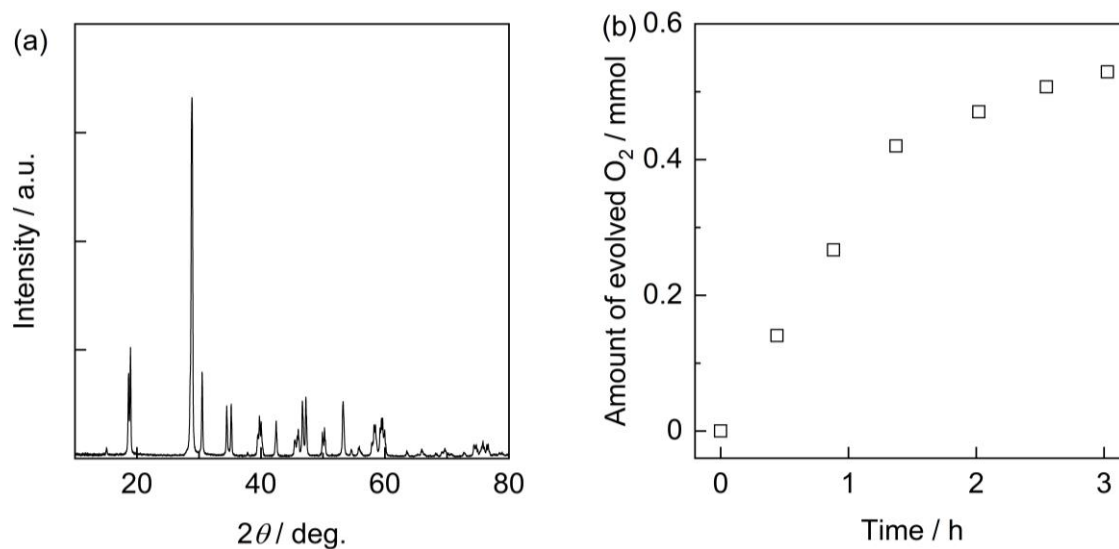


Fig. S8. (a) The XRD pattern obtained from Mo:BVO^{3,4} particles and (b) the time course of oxygen evolution from an aqueous solution containing a sacrificial electron acceptor and Mo:BVO with white light illumination instead of monochromatic light. Reaction conditions: photocatalyst = 0.2 g, aqueous solution = 200 mL of 10 mM AgNO₃, light source = 300 W Xe lamp ($420 < \lambda < 800$ nm).

Electronic Supplementary Information

The appearance of the experimental setup is shown in Fig. S8a. The reaction vessel connected to the glass closed gas circulation system was completely covered with the aluminum foil to minimize the undesired loss of the incident photons. On the other hand, Mo:BVO and DPA-PtOEP-Sumecton showed relatively high dispersibility in water as shown in Fig. S8b. It should be noted that the host material, Sumecton, shows high transparency as well and thus does not interfere with the light absorption of PtOEP as well as light emission from DPA. Therefore, incident photons should eventually reach the upconverting composites through the scattering, while the blue emission light can also easily approach Mo:BVO photocatalysts.

The calibration curve (amounts of oxygen vs. area of thermal conductivity detector (TCD) signal assigned to oxygen) utilized for the photocatalytic experiments is provided in Fig. S9. They showed clear linear relationship with quite high R^2 value. In the present study, all photocatalytic experiments shown in Fig. 5 of the main manuscript (Mo:BVO w/ DPA-PtOEP-Sumecton, w/ PtOEP-Sumecton and w/o Sumecton) were conducted with using the same reaction vessel connected to the same glass closed gas circulation system and the same gas chromatography equipped with TCD detector, as well as the same light source. Therefore, the variations in the photocatalytic activities shown in Fig. 5 simply reflects the area of TCD signal as shown in Fig. S10.

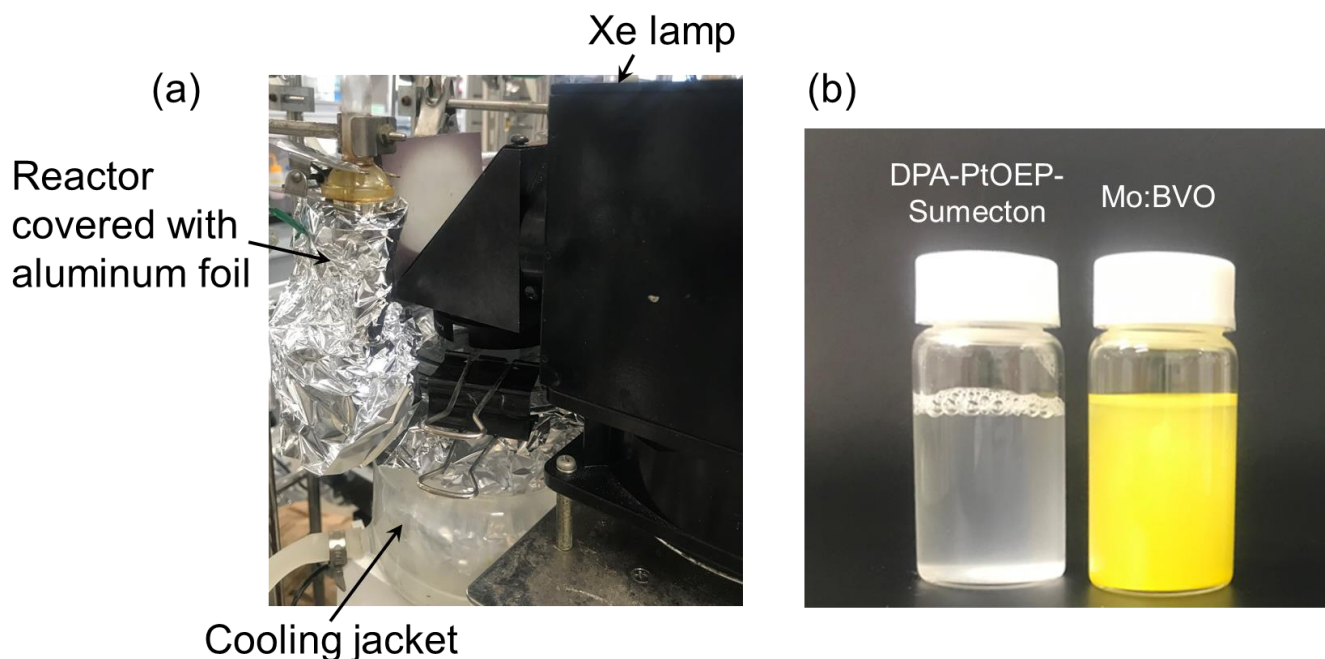


Fig. S9. (a) Appearance of the experimental setup for the photocatalytic reaction. The reaction vessel covered with the aluminum foil was connected to the glass closed gas circulation system and illuminated from top-side by the Xe lamp. (b) Photographic image of aqueous dispersion containing DPA-PtOEP-Sumecton or Mo:BVO with concentration of 1 g of particulate materials per 1 L of water.

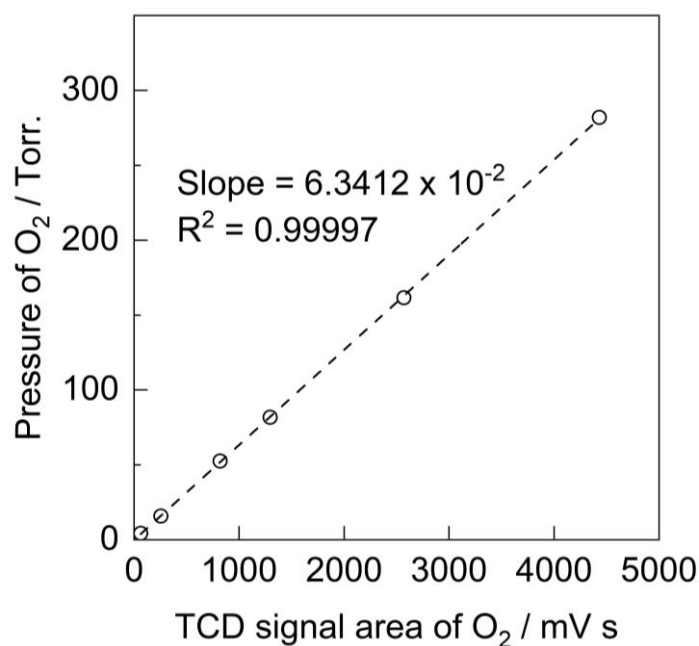


Fig. S10. Calibration curve utilized for the photocatalytic experiments shown in the main manuscript.

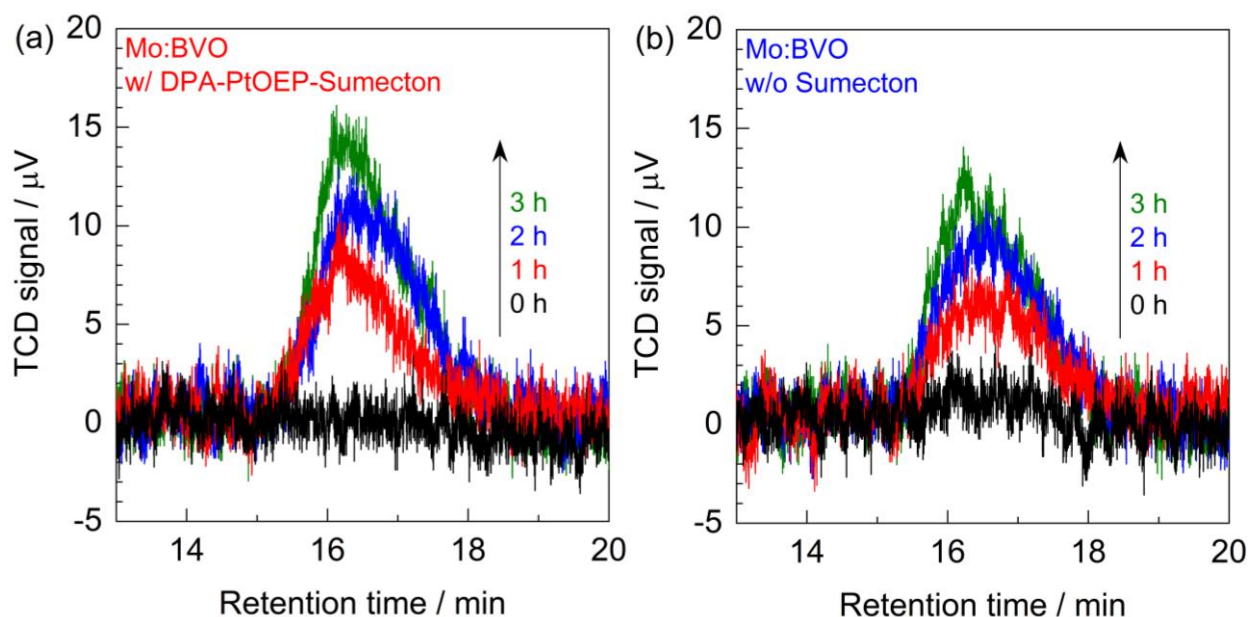


Fig. S11. Gas chromatograms obtained during the photocatalytic oxygen evolution reaction by (a) Mo:BVO w/ or (b) w/o DPA-PtOEP-Sumecton upconverting composite under 0–3 h of light illumination.

References

- 1 K. Yano, A. Usuki and A. Okada, *J. Polym. Sci. Part A Polym. Chem.*, **1997**, 35:2289–2294.
- 2 F. Kishimoto, T. Wakihara and T. Okubo, *ACS Appl. Mater. Interfaces*, **2020**, 12, 6, 7021-7029.
- 3 A. Iwase, H. Ito, Q. Jia and A.; Kudo, *Chem. Lett.*, **2016**, 45, 152–154.
- 4 A. Kudo, K. Omori and H. Kato, *J. Am. Chem. Soc.*, **1999**, 121, 11459-11467.